Chapter 4

3D Woven Composites: From Weaving to Manufacturing

Hassan M. El-Dessouky and Mohamed N. Saleh

Additional information is available at the end of the chapter

http://dx.doi.org/10.5772/intechopen.74311

Abstract

Manufacturing near-net shape preforms of fibre-reinforced composites has received growing interest from industry. Traditionally, a preform was made from 2D fabrics, but recently, it has been shown that 3D textiles can be used with success; with weaving being the predominant technology for carbon fibre composites. In 3D weaving, weft, warp and binder fibres run across, along and through the fabrics in the X, Y and Z directions, respectively. Producing a unitised single-piece fabric and subsequently reducing the takt time required for rapid composite manufacturing are two of the main advantages of using 3D woven preforms. Weaving of 3D fabrics, manufacturing of 3D composites, physical characterisation and mechanical testing of infused composites samples are discussed in this chapter. Finally, a large automotive composite made of single-piece 3D woven preform was manufactured and presented for demonstration.

Keywords: 3D woven composites, carbon fibre, manufacturing, mechanical properties, resin transfer moulding (RTM)

1. Introduction

Two-dimensional (2D) laminated composites are characterised by their in-plane high specific stiffness and strength [1]. However, many real life applications are exposed to out-of-plane loading conditions that make it impossible to resort to the 2D laminates as the proper solution. Wind turbine blades, stringers and stiffeners in aircraft, pressure vessels and construction applications are some examples of applications in which out-of-plane loading conditions are imposed on the structure. Thus, the need for composite materials with enhanced through-thickness "out-of-plane" properties has emerged. This need requires replacing

2D laminated composites with three-dimensional (3D) textile structures. The "enhanced out-of-plane properties" is not the only advantage of 3D composites. The delamination resistance, due to the z-binder existence, enhances the impact performance and damage tolerance of such material systems [2]. In addition, using textile technology can be utilised to manufacture near-net-shape preforms. So, it reduces the manufacturing/machining cost and time even further. Although various techniques exist for manufacturing 3D textile preforms, the most widely used nowadays is weaving due to its high production rate along with the ability to produce various 3D woven structures [1]. In terms of the energy consumption required for textile production, it depends very much on the type of the yarn and the weaving pattern. For example one of the published studies entitled "Material Intensity of Advanced Composite Materials" [3], reported that the average figure for the electricity consumption is approximately 0.11 kWh per m^2 for glass fibres and 0.214 kWh/m^2 for carbon fibres.

Generally, 3D woven composites can be divided into two main groups depending on how deep the binder penetrates through the fabric. If it penetrates all the way through the thickness it is referred to as through-thickness (TT) interlock (see **Figure 1a, c**) while it is classified as layer-to-layer (LTL) if the binder only holds adjacent layers (see **Figure 1b**). Then this classification is further divided according to the interlacing angle of the structure. The first category is the angle interlock (AI) in which the interlacing angle between the binder and weft yarns can have any value except 90° (**Figure 1c**). The second category is a special case of the first one. The orthogonal interlock (ORT) (**Figure 1a**) occurs when the interlacing angle between the binder and weft yarns is equal to 90° [1].

The weave pattern used during the weaving process can also affect the classification of 3D woven composites. For instance in the case of ORT weave, the frequency of the z-binder sweeping the top and bottom surfaces of the weave can vary from plain (**Figure 2a**) to twill (**Figure 2b**) or satin (**Figure 2c**) pattern. This will directly affect the unit-cell size, degree of crimp, elastic response and damage/delamination resistance as highlighted previously in [4–6].

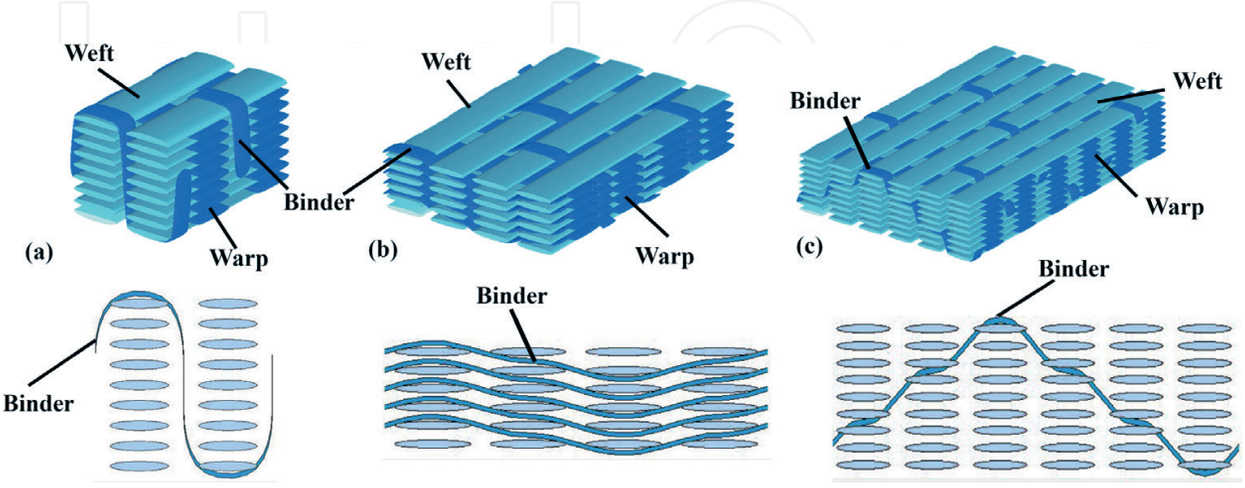

Figure 1. Types of 3D woven composites based on the binder path: (a) ORT, (b) LTL and (c) AI [4].

http://dx.doi.org/10.5772/intechopen.74311

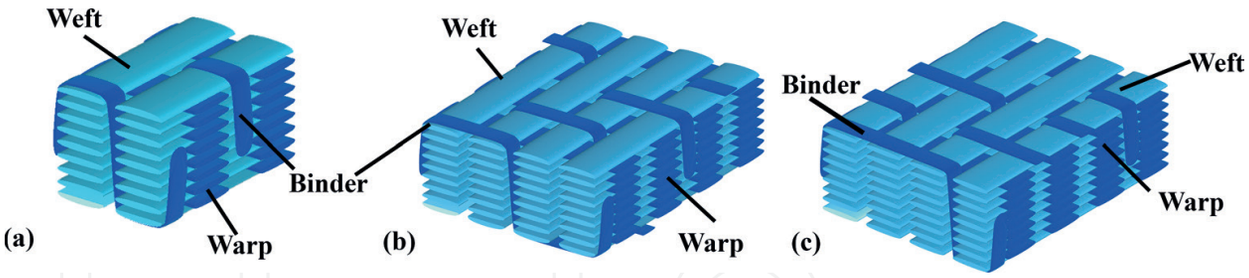

Figure 2. Examples of possible weave binding patterns for ORT: (a) plain, (b) twill and (c) satin [4].

The applications of 3D woven composites have been growing tremendously in industry recently [7–9]. In applications that require load transfer around a bend such as curved beams, T-joints and brackets, 3D woven AI and LTL architectures have been utilised [10]. The main advantages observed for these architectures are that they have better interlaminar shear and radial stress resistance. In addition, McClain [2] reported successfully using 3Dwoven AI and LTL architectures in truss beams with integrated off-axis stiffeners. Applications [2] in which continuous fibres are required for joining skin and stiffening elements as well managed to utilise those previously highlighted architectures, and consequently overcoming the need for bonding or fastening composite parts which is one of the major challenges facing 2D laminated composite nowadays. 3D woven LTL composites have been utilised in the automotive industry [11–13]. Not only LTL and AI woven composites have managed to find their way into industry, but also their ORT woven counterparts. For example, Bayraktar et al. [11] reported using ORT woven composites to replace high-strength steel beams. Hemrick et al. [14] reported the use of ORT woven composite in ultra-light weight heat exchangers in the automotive industry. The concept utilises the high thermal conductivity of ORT woven composites due to the through-thickness binding yarns creating a conduction path for the heat to dissipate. Moreover, ORT woven composites have been successfully employed in the LEAP project to manufacture engine casings and fan blades for A-320-neo, 737-MAX and Comac C-919 [15].

Considering the environmental impact, the technique presented in this study can be used to weave recycled carbon fibre yarns. There are commercially available yarns produced from recycled short carbon fibre. However, from structural and strength point of view, these yarns are not recommended to be used as the principal reinforcing material in FRP composites. They can still be used as a secondary material. For instance, along the warp direction in a weaving process, continuous carbon fibre yarns can be used as the principal material while the recycled carbon fibre yarns can be used as a secondary material along the weft direction depending on the loading experienced by the structural component.

In this chapter, a case study on manufacturing a complex automotive part from 3D composite is discussed. Considering the fabric drapeability and conformity, one of the most common 3D woven architectures, LTL weave is considered in this study. The design and weaving of three weave patterns of LTL: plain, twill and satin weaves (LTL-PW, LTL-TW and LTL-SW) are presented. Flat composite panels are manufactured using resin transfer moulding (RTM). The quality and integrity of the manufactured composite samples are physically characterised

through optical microscopy, density measurements, voids content and fibre volume fraction analysis. To observe the differences in mechanical properties between the different LTL weave designs, composite samples are mechanically tested to failure using tensile and flexure 3-point bending tests. The possibility of manufacturing a large and complex automotive component of multi-weave (LTL-PW, LTL-TW & LTL-SW) composite is demonstrated.

2. Experimentation

2.1. Weave design

Recently developed weave-design software (EAT-3D Module) for composite structures is used to design LTL plain, twill and satin weaves; each of which contains five warp and five weft layers. All weaves were designed with the same drafting plan to weave fabrics with the same loom setup and change weave designs within the same piece of fabric to produce a multi-weave preform. **Figure 3** demonstrates the schematic of the three different fabrics, with the warp yarns highlighted in blue, the weft yarns are in red and the through thickness binders are shown in green.

A Dornier double-rapier FT-Dobby loom was used in this study. The machine was commissioned to weave conventional 2D fabrics, but it has been recently modified to weave 3D structures (See **Figure 4**). A creel of 912 positions was loaded with T300-6 k carbon fibre bobbins to warp the loom. The creel is equipped with central tension control to alter the tension of warp and binder during the weaving process. **Figure 4** shows the setup of weaving machine (loom & creel) used to weave the 3D weave designs mentioned above. Considering the configuration of the automotive demonstrator (750 × 700 × 2 mm) and the creel number of ends (912) available, the densities in the warp and the weft were set up to 12.66 ends/cm and 21.00 picks/cm respectively. The unbalanced fabric sett or density allows better handle-ability, stability and transferability of woven preforms that is not achievable in the case of the balanced sett.

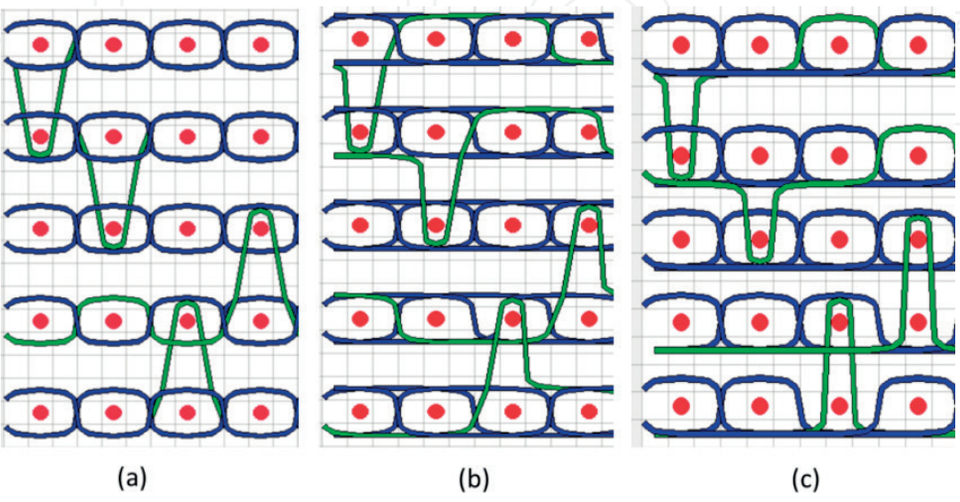

Figure 3. Schematic cross-sections of weaves designed: (a) LTL-PW, (b) LTL-TW and (c) LTL-SW.

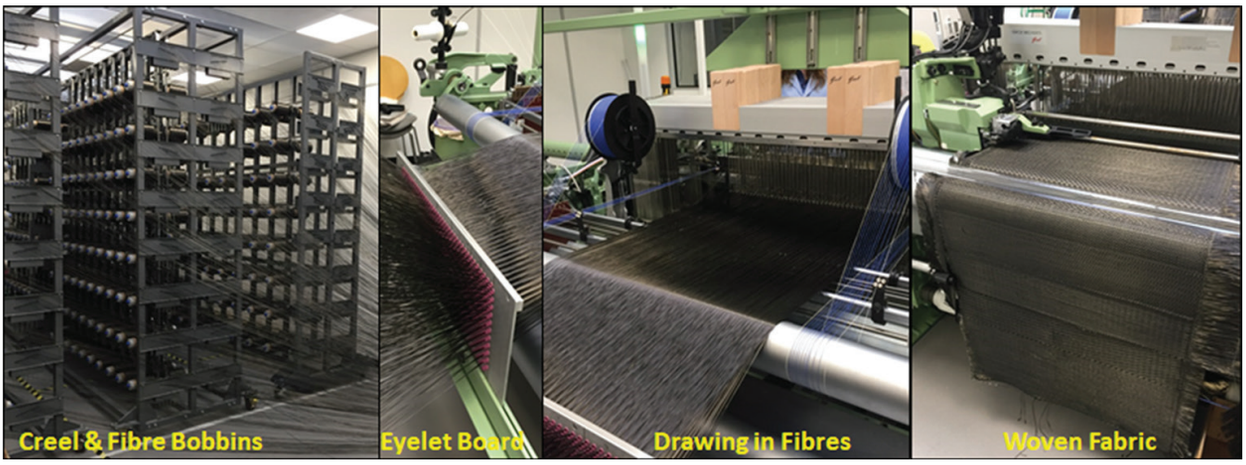

Figure 4. Weaving setup.

All fabrics produced have approximately the same areal density (~1350 gsm) to ensure fibre volume fraction (~50%) in the final composite.

2.2. Composite panels manufacturing

A resin transfer moulding (RTM) tool of 320 × 310 mm was used to manufacture flat composite panels. Gurit T-Prime 130-1 epoxy was used and mixed at: 100/27 by wt% of resin/hardener. The density of the cured resin was measured to be 1.156 g/cm^3. The laminate thickness was designed to be 1.5 mm. Heater pads were positioned on the outside of the tool to heat it. The tool was preheated to 80°C. Prior to injecting the resin, it was degassed in a degassing chamber for 30 min, and then placed in a pressure pot. The resin was injected at 2 bars of pressure, and −1 bar of vacuum was attached to the outlet tube. When the resin had fully wetted the preform the outlet pipe was clamped, the pressure was left on for a further 15 min to ensure the entire mould had an even pressure and compaction and that any air bubbles would shrink to reduce voids in the final composite. The panels were left to cure in the mould for 1 hour at 80°C after the outlet pipe was clamped.

2.3. Physical characterisation of composite samples

2.3.1. Density, fibre volume fraction and void content

In order to examine the quality and integrity of the manufactured composite, physical characterisation of the RTM panels was conducted. The fibre-volume fraction (V_f) analysis was carried out in accordance with ASTM D 3171 standard [16]. A minimum of 6 specimens were cut from random locations from the cured laminates resulting in total of 18 specimens for the three different architectures. According to the ASTM standard, the minimum weight of each specimen has to be 1 g to be able to determine the void content, so specimens' weight in this study was approximately 1.2 g. The density of the specimens was determined, before the burn-off, using AccuPyc II 1340 Gas Pycnometer from micromeritics. Then, the furnace was adjusted at 600°C and the burn-off duration for each specimen was approximately 25 min. The calculation of fibre, matrix and voids content (%) is depicted as follows:

$$V_f = \left(M_f / M_i\right) \times \left(\rho_c / \rho_r\right) \times 100 \quad (1)$$

$$V_m = \left(M_i - M_f\right) / M_i \times \left(\rho_c / \rho_r\right) \times 100 \quad (2)$$

$$V_v = 100 - \left(V_f + V_m\right) \quad (3)$$

where M_i is the initial mass of specimen before burn-off, g, M_f is the final mass of specimen after burn-off, g, ρ_r is the density of the reinforcement/fibre, g/cm^3, ρ_c is the density of the composite specimen, g/cm^3, ρ_m is the density of the matrix, g/cm^3, V_f is the fibre volume percentage, V_m is the matrix volume percentage, V_v is the voids volume percentage.

Table 1 lists the V_f analysis results. The volume of voids (V_v) in all composites was found to be negative. This can be attributed to the experimental error during the V_f analysis, which suggests that the manufactured panels for all 3D woven fabrics were free from voids. Optical microscopy images support this observation as discussed later in this section.

2.3.2. Optical microscopy

Using two-part epoxy compound the composite specimens (20 × 20 mm) were cured in 30 mm diameter resin blocks. The polishing procedure was as follows: silicon carbide SiC-220 for 20 s and SiC-1200 for 2 min until flat, 9-μ (MD-Plan) for 4 min, 3-μ (MD-Dac) for 4 min and OP-S for 2.5 min plus 1 min on water to clean OP-S off. Rotation speed was 150 rpm and applied force per sample was 30 N. Alicona-IFM-G4 microscope was used to optically scan the polished sections and optical images were captured for illustration.

Figure 5 depicts the optical cross-sections of the three composite laminates across weft direction (top image) and across warp direction (bottom image); (a) LTL-PW, (b) LTL-TW, and (c) LTL-SW. The arrangement of weft, warp and binder tows is marked (see **Figure 5**) for clarification.

To further investigate the composite's integrity, wettability and porosity, **Figure 6** shows a selection of the zoomed-in optical images taken from the cross-sections displayed in **Figure 5** for the three LTL weaves plain, twill and satin respectively. The optical cross-sections were captured along the warp (left) and weft (right) directions. No voids were observed which suggests that the binding yarns behaved as channels for the resin to follow during the

Property/weave	LTL-PW	LTL-TW	LTL-SW
Density (g/cm^3)	1.438 ± 0.005	1.456 ± 0.017	1.464 ± 0.006
V_f (%)	46.51 ± 0.66	48.12 ± 1.05	48.71 ± 0.46
V_v (%)	−0.06 ± 0.35	−0.70 ± 0.96	−1.24 ± 0.40

Table 1. Results of the fibre volume fraction analysis.

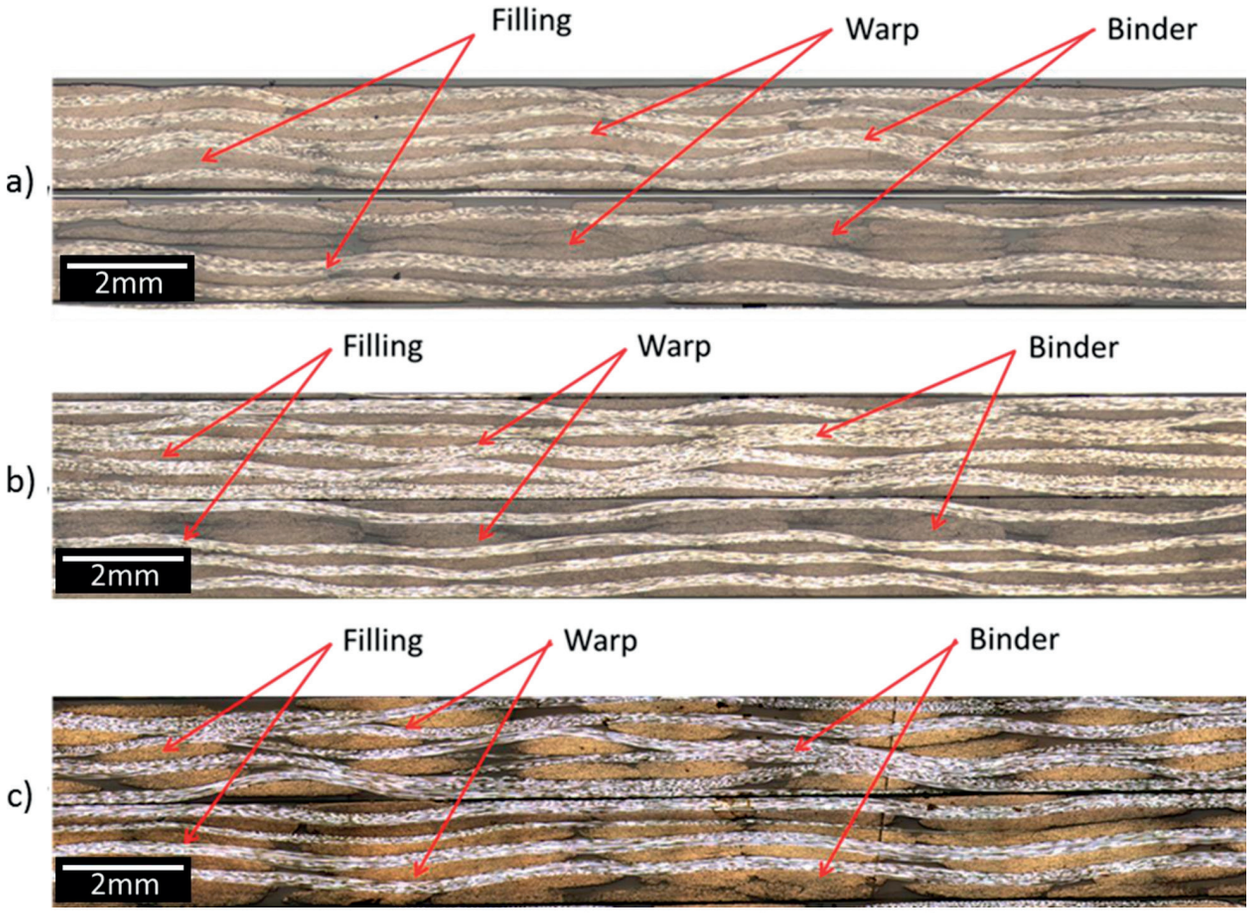

Figure 5. Optical cross-sections of the composite laminates at a low magnification: (a) LTL-PW, (b) LTL-TW and (c) LTL-SW.

infusion process. On the other hand, the existence of binding yarns in 3D woven architectures creates resin rich areas (RRA) in the cured composite. RRA, present between yarns, have been reported as one of the drawbacks of using 3D woven composites as they allow cracks to propagate quickly and cause failure at specific locations in the fabric architecture upon loading [17].

2.4. Mechanical testing

Mechanical testing was carried out to observe the differences in mechanical properties between the different weave designs. The composite laminates manufactured by RTM were mechanically tested to failure using tensile and flexure 3-point bending tests at AMRC Advanced Structural Testing Centre (ASTC). These two tests were chosen to represent some of the different loading conditions that a composite part may experience to during its commercial use. All the tests were carried out in the warp and weft direction as each direction exhibits different properties due to the fibre counts and orientations in each direction. Six specimens were tested for each direction to assure repeatability. All the specimens had a thickness of approximately 1.5 mm.

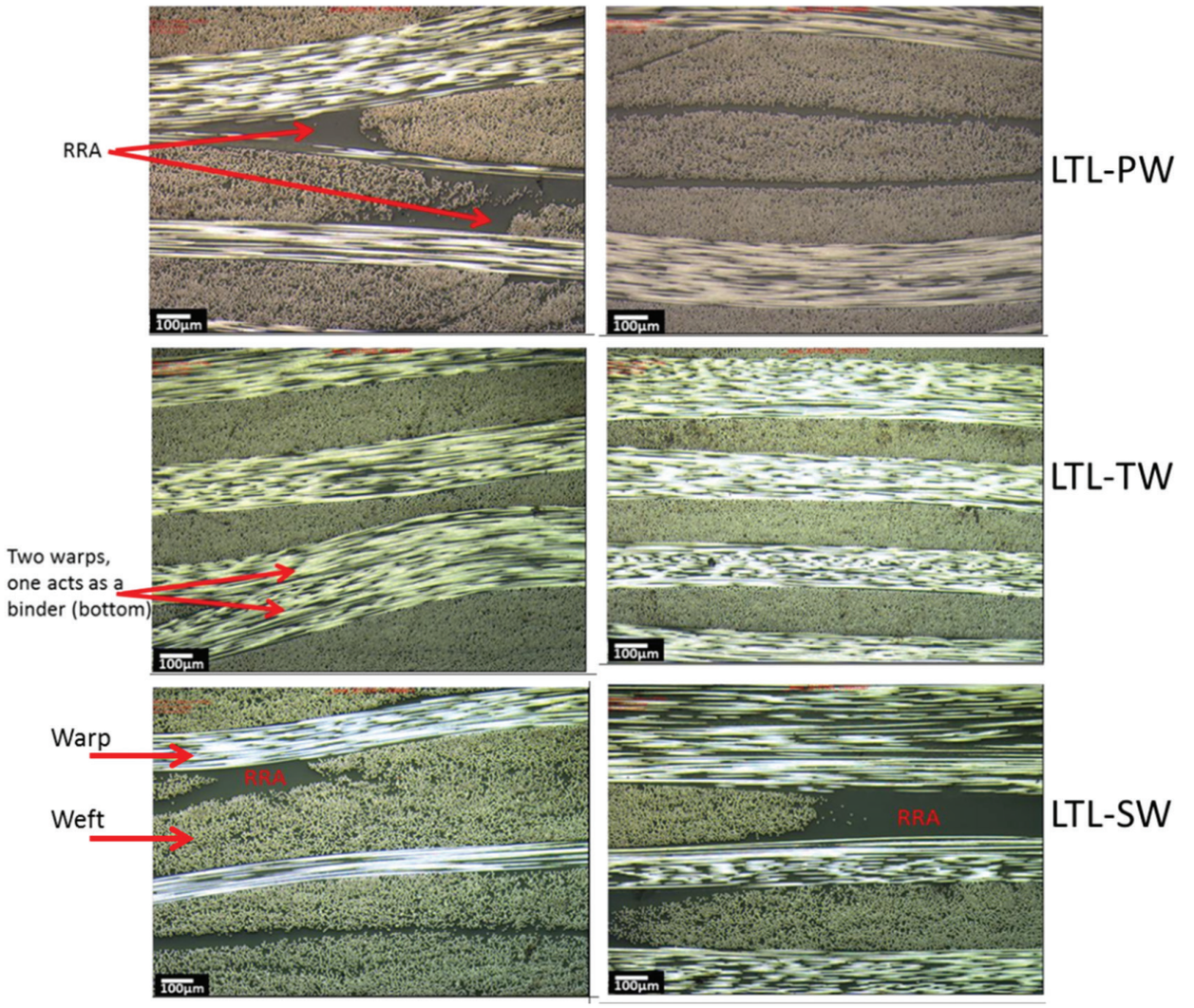

Figure 6. A selection of optical cross-sections of the composite samples at a higher magnification across the weft (left) and warp (right) directions.

In the tensile and flexural results a general observation is the modulus and strength results in the weft direction are significantly higher in comparison to the warp direction for all the fabrics. This could be attributed to two main reasons; (i) the directional V_f whereby the V_f in the weft direction is almost double the V_f in the warp direction, (ii) the warp yarns experience higher crimp due to the interlacement points between the layers making them susceptible to localised stress leading to premature localised damage and ultimate failure. These reasons are further highlighted in the following sections in the summary tables for the modulus and strength results.

2.4.1. Tensile testing

Following ASTM D3039, tensile tests were carried out. **Figure 7** shows the tensile stress–strain graphs for each material including the test setup. The graphs show the repeatability of the test

in each direction. The warp specimens are highlighted as solid lines and the weft specimens as dashed lines.

Tables 2 and **3** summarise the tensile results in the warp and weft direction along with the directional V_f. In both the warp and weft direction the LTL-PW composite performed the least in strength and modulus. Within the plain weave fabric the yarns are undergoing constant undulation. This undulation creates more interlacement points within the fabric which affects the modulus in the linear elastic regime and during the tensile extension the interlacing points create localised stress affecting the ultimate strength.

The LTL-SW demonstrated the highest modulus in the warp and weft directions. This is due to the directional V_f which is higher in the LTL-SW compared to the other weaves as it contains the least amount of crimp.

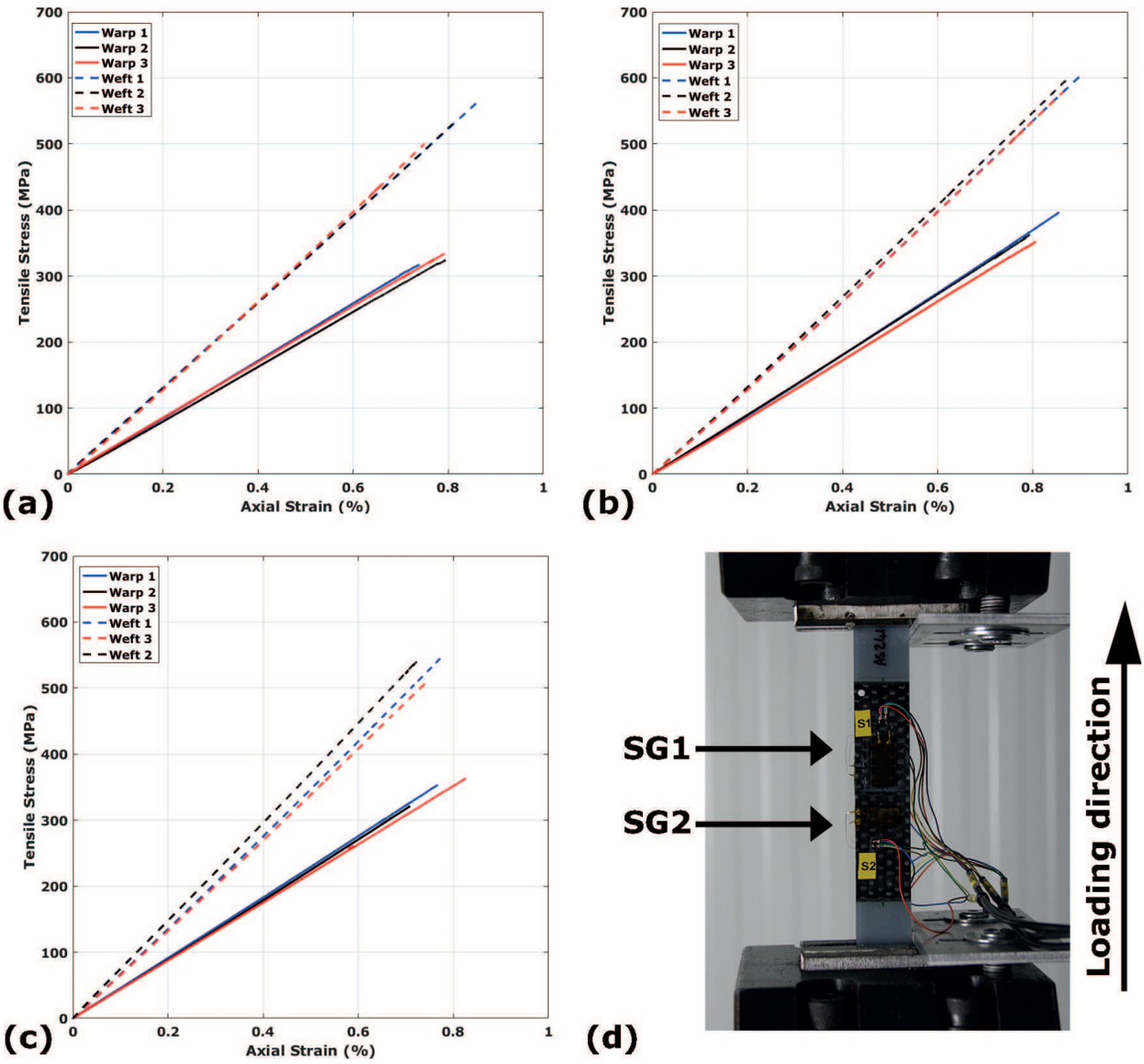

Figure 7. (a–c) Tensile stress–strain graphs: (a) LTL-PW, (b) LTL-TW, (c) LTL-SW and (d) test setup.

Warp direction	V_f (%)	Modulus (GPa)	Tensile strain (%)	Tensile strength (MPa)
LTL-PW	17.50 ± 0.25	41.25 ± 1.49	0.83 ± 0.08	335.26 ± 15.24
LTL-TW	18.11 ± 0.39	44.20 ± 0.98	0.80 ± 0.04	359.56 ± 22.45
LTL-SW	18.33 ± 0.17	51.52 ± 9.56	0.69 ± 0.11	345.47 ± 15.80

Table 2. Tensile results in the warp direction.

Weft direction	V_f (%)	Modulus (GPa)	Tensile strain (%)	Tensile strength (MPa)
LTL-PW	29.01 ± 0.41	63.46 ± 3.18	0.82 ± 0.05	525.86 ± 24.08
LTL-TW	30.01 ± 0.65	67.74 ± 2.38	0.84 ± 0.06	582.89 ± 32.78
LTL-SW	30.38 ± 0.29	70.99 ± 2.54	0.79 ± 0.07	575.11 ± 65.96

Table 3. Tensile results in the weft direction.

The failure strain of the fibre used (12 k-T300) is 1.5%. The measured failure strain from the test was 50% lower due to the interlacing nature between warp and weft yarns within the fabrics. It is possible that higher localised stress/strain than measured was experienced, at the interlacements or the matrix RRA, causing failure of the coupons. Saleh et al. [6] used a digital image correlation system during tensile testing which showed areas where interlacement points occurred to experience high strain values near failure of the coupon.

2.4.2. Flexure testing

Using ASTM D7264, 3 point bending flexure tests were carried out. The flexure stress–strain curves of all the tested architectures are represented in **Figure 8** along with the test setup. In the graphs the warp results are plotted as solid lines and the weft results as dashed lines. The graphs show good repeatability between the repeats in each direction. As expected, all specimens behave in a linear elastic manner up to failure as they are loaded along the fibre direction, in either the warp or weft direction.

Tables 4 and **5** summarise the flexural properties obtained in correspondence with the V_f in both directions, warp and weft.

The flexural modulus of composite materials is a function of the composite lay-up/ stacking sequence. More precisely, it is a function of how far the aligned plies with the loading direction are from the mid-plane of the cured laminate as well as the volume fraction in this specific direction. Ideally for isotropic materials, the flexure modulus should not differ from the tensile modulus for the same material such as metals, however practically this is not the case especially in the case of fibre reinforced polymers because of their orthotropic nature. Thus, flexure testing is not ideal for determining the modulus and it is recommended that the tensile modulus is used over the flexural modulus.

As a general remark, the main difference between the flexure test and the tensile test in this study is that the tested specimen in the case of flexure testing experiences both tensile and

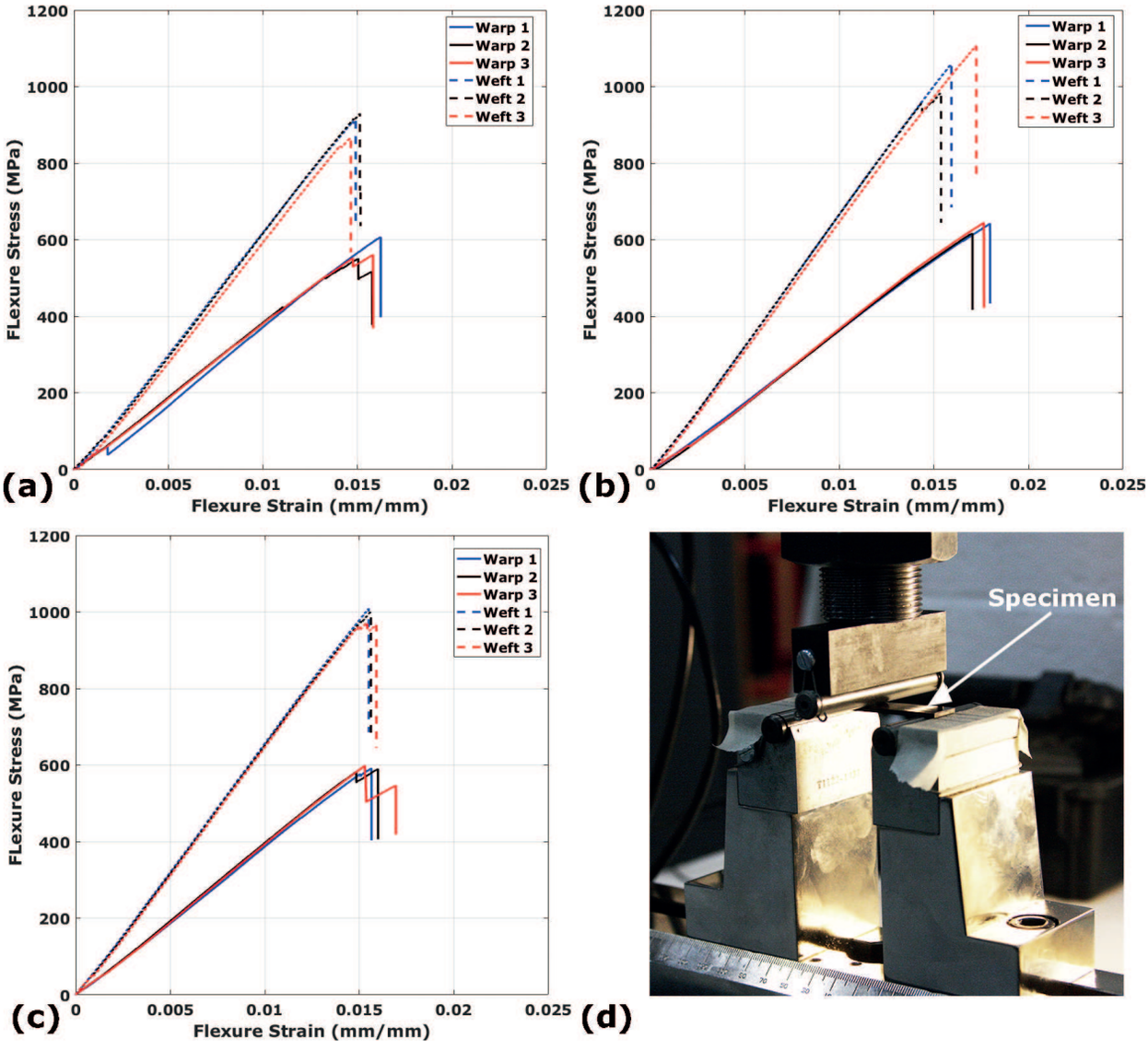

Figure 8. (a-c) Flexure stress–strain graphs: (a) LTL-PW, (b) LTL-TW, (c) LTL-SW and (d) test setup.

compressive stresses in the lower and the upper surfaces respectively due to the nature of the imposed loading condition. So, it is not straight forward to determine the reason behind final fracture as it might be a mixed mode. It seems there is a trend in the obtained results, but it is difficult to justify this behaviour without carrying out a detailed damage propagation investigation by different techniques such as X-ray CT, optical microscopy or acoustic emission techniques.

Warp direction	V_f (%)	Modulus (GPa)	Flexural strain (%)	Flexural strength (MPa)
LTL-PW	17.50 ± 0.25	35.58 ± 5.19	1.53 ± 0.10	574.07 ± 30.31
LTL-TW	18.11 ± 0.39	33.99 ± 2.91	1.73 ± 0.10	644.88 ± 51.72
LTL-SW	18.33 ± 0.17	35.16 ± 2.18	1.56 ± 0.02	573.27 ± 37.43

Table 4. Flexural results in the warp direction.

Weft direction	V_f (%)	Modulus (GPa)	Flexural strain (%)	Flexural strength (MPa)
LTL-PW	29.01 ± 0.41	57.48 ± 2.46	1.48 ± 0.02	902.30 ± 19.58
LTL-TW	30.01 ± 0.65	62.84 ± 2.14	1.54 ± 0.10	996.42 ± 64.00
LTL-SW	30.38 ± 0.29	61.49 ± 2.44	1.53 ± 0.09	968.21 ± 65.16

Table 5. Flexural results in the weft direction.

3. Composite demonstrator manufacturing

The use of 2D fabrics in composite preforming applications is well established but there are two major deficiencies, the lack of reinforcement through thickness and labour cost, which drive the interest towards using 3D woven preform in high volume manufacturing such as automotive. Therefore, an automotive floor section made of 3D woven fabric is selected to be demonstrated. Traditionally such component (**Figure 9a**) was made of three discrete 2D preforms leading to some drawbacks such as: (i) preforms overlap, (ii) discontinuous fibres along the component, (iii) interlaminar delamination and (iv) labour time consuming. Considering the complex geometry of the demonstrator and to overcome the drawbacks of 2D fabrics, a drapeable and single –piece 3D woven preform is required to conform well to the intricate features of the demonstrator. The LTL architecture could be a suitable solution.

The fabric designed and produced for the generic automotive part was made up of 5 zones; each zone was made of a specific weave to suit the conformity of the area on the mould. For areas requiring high conformity (**Figure 9b**, zone 3), a satin weave was considered. The area (**Figure 9b**, zone 2) requires a medium conformity, so a twill weave was suggested. Whereas an area with low conformity (**Figure 9b**, zone 1) a plain weave was nominated. The preform of varying drapeable weave allows the fabric to conform to the mould and prevents the fabric from wrinkling.

The RTM mould of the generic automotive part was designed and manufactured from aluminium (**Figure 10**) and used to perform RTM injections of the fabric woven. The parts were injected from one inlet in the top half of the mould and four outlet points were positioned in each corner, on the bottom of the mould.

To preform and cut the 3D multiweave fabric, a template was used to hold the fabric in the correct position and shape whilst the fabric was cut. This method prevented the fabric from moving whilst being cut. Once the fabric was cut it was crucial not to move the fabric to prevent the fabric from fraying and distortion.

As with the flat panels, Gurit T-Prime 130-1 resin and hardener was used. The parts were injected at room temperature and placed in the oven after injection to cure at 80°C. During the injection −1 bar of vacuum was applied to the outlet, whilst the resin at the inlet was under pressure. At 2 bar of pressure the mould took 25 min for the resin to exit all the outlets and

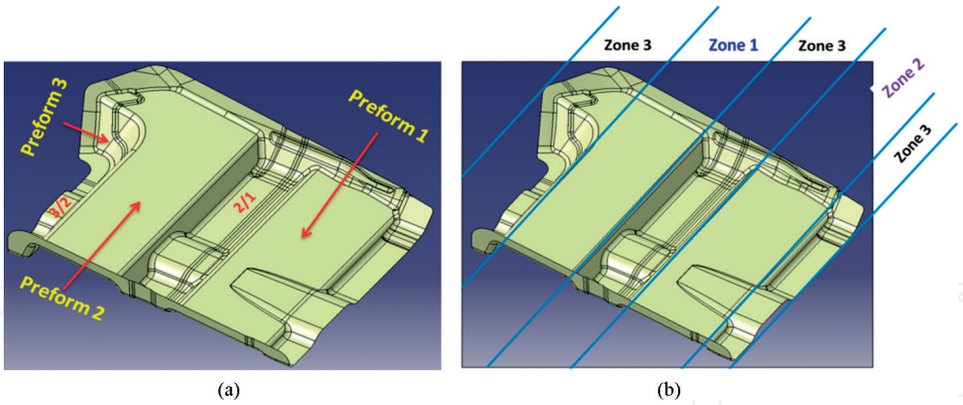

Figure 9. CAD of generic automotive component, (a) the use of three types of 2D preforms and (b) the use of a single 3D woven preform.

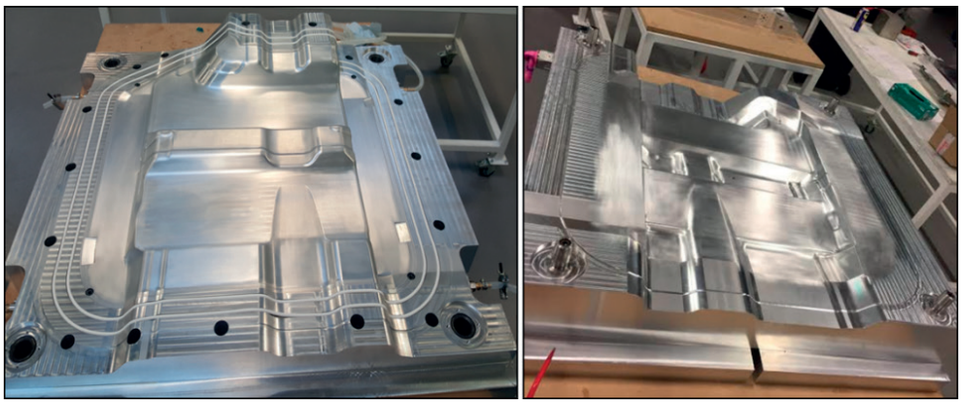

Figure 10. RTM mould: Male (left) and female (right) tools.

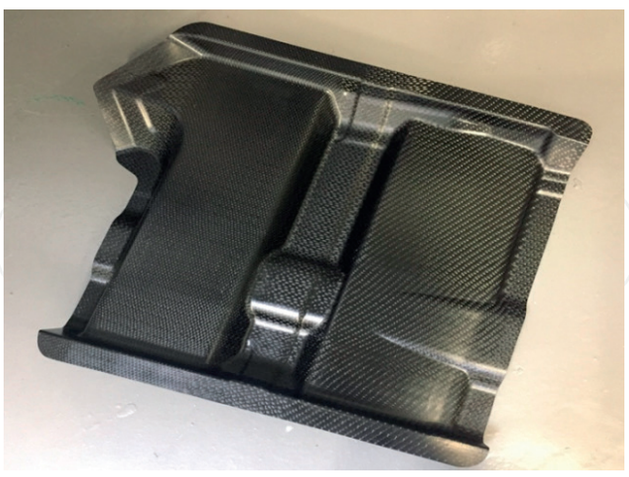

Figure 11. Automotive composite RTM cured part.

the pressure and inlet was left open for a further 30 min. Whereas at 3.5 bar of pressure the mould took 12 min for the resin to exit all the outlets and the pressure and inlet was left open for a further 22 min.

One of the successful RTM parts is demonstrated in **Figure 11**. Further investigations of the cured composite component are required to assess the quality of the RTM part and to determine the fibre volume fraction and voids content alongside with optical scans.

4. Conclusion

A standard loom equipped with a cost-effective shedding system, Dobby not Jacquard, was successfully used to weave 3D complex architectures. The density measurements and optical microscopy revealed that the RTM composite laminates made were voids free.

In the mechanical testing, the tensile and flexural results showed that the modulus and strength to be significantly higher in the weft direction. It is believed the difference is due to differences in the directional V_f and that the warp yarns experiencing significantly higher crimp. The LTL plain fabric exhibited the lowest mechanical properties due to the constant undulation and cross over points between the yarns in the fabric. It is thought that the cross over points created areas of high localised stress leading to earlier failure of the composite coupons. The LTL twill and satin fabric performed fairly similar to each other. The two fabrics had the same amount of cross over points (interlacing) between the warp and the weft, which was less than the plain woven fabric. Due to less crossover points in the fabrics, there were less areas of localised stress allowing the coupons to withstand higher loads.

Final fabric was woven with multiple zones made up of different weave patterns. The different zones corresponded to different areas on the generic automotive part to suit the varying conformity of the part. The fabric conformed well to the RTM tool and successful part was demonstrated.

5. Current limitations and future trends

There are still some limitations in the process of 3D weaving of carbon fibre for manufacturing composites. Two of the main limitations are the heavy tow weaving and the fibre orientation. Heavy tows more than 24 k are difficult to weave using conventional weaving machines. Moreover, fundamentally in weaving, the warp yarns run in one direction (x-direction) while the weft yarns run in the transverse direction (y-direction). Thus, it is quite challenging if different orientations for yarns are required to produce a multiaxial or off axis fabrics for instance. There are some research-scale weaving looms that are customised to produce biased 3D weaving but yet is commercialised to date.

Currently, 3D weaving represents an automated process which can provide through thickness reinforced composites at high laydown rates using fibrous materials in their least value added form. It therefore offers the ability to add functionality, reduce cost and hit rate requirements for high volume manufacture of composites compared to traditional 2D approaches. These benefits exist in the woven fabric itself, but to mechanically convert this fabric into a useable preform for a composite moulding operation, a number of solutions are required such as

thickness tapering, stabilisation & edge trimming. These additional processes add extra flexibility by moving the manufacturer from a weaver of fabric to a producer of composite preforms tailored to match performance specifications, therefore adding significant extra value. Current add-on processes often involve a number of slow manual operations to convert the fabric into a preform and, in many cases, also distort or damage it. Thus, the ultimate goal of weaving of 3D woven fabrics development is to achieve integrated manufacturing process via automation to overcome the slow manual operations in the composites' supply chain.

Acknowledgements

Authors would like to acknowledge the collaboration with the UK Catapult centres Manufacturing Technology Centre (MTC), National Composites Centre (NCC) and Warwick Manufacturing Group (WMG). Special thanks to AMRC composite centre staff involved: Alice Snape, Jody Turner, Hannah Tew and Richard Scaife.

Conflict of interest

The authors declare that they have no conflict of interest.

Author details

Hassan M. El-Dessouky[1,2,3]* and Mohamed N. Saleh[1]

*Address all correspondence to: hassanoptics@yahoo.com

1 Composites Centre, AMRC with Boeing, University of Sheffield, UK

2 Department of Fashion and Textiles, University of Huddersfield, UK

3 Physics Department, Mansoura University, Egypt

References

[1] Ansar M, Xinwei W, Chouwei Z. Modeling strategies of 3D woven composites: A review. Composite Structures. 2011;**93**:1947-1963. DOI: 10.1016/j.compstruct.2011.03.010

[2] Mcclain M, Senior R, Organic TE, Composites M. Overview of recent developments in 3D structures. Albany Engineered Composites. 2012:1-12

[3] Stiller H. Material Intensity of Advanced Composite Materials. Wuppertal: Wuppertal Institute for Climate, Environment and Energy; 1999

[4] Saleh MN, Soutis C. Recent advancements in mechanical characterisation of 3D woven composites. Mechanics of Advanced Materials and Modern Processes. 2017;**3**. DOI: 10.1186/s40759-017-0027-z

[5] Saleh MN, Wang Y, Yudhanto A, Joesbury A, Potluri P, Lubineau G, et al. Investigating the potential of using off-Axis 3D woven composites in composite joints' applications. Applied Composite Materials. 2016;**24**:377-396. DOI: 10.1007/s10443-016-9529-9

[6] Saleh MN, Yudhanto A, Potluri P, Lubineau G, Soutis C. Characterising the loading direction sensitivity of 3D woven composites: Effect of z-binder architecture. Composites. Part A, Applied Science and Manufacturing. 2016;**90**:577-588. DOI: 10.1016/j.compositesa.2016.08.028

[7] McHugh C. Creating 3-D, One Piece, Woven Carbon Preforms Using Conventional Weaving and Shedding. SAMPE Conf. vol. 45; 2009. pp. 33-41

[8] McHugh C. The Manufacture of One Piece Woven Three Dimensional Carbon Fiber Nodal Structures. SAMPE Conf.; 2010

[9] Chen X, Chen X, Taylor LW, Tsai L. An overview on fabrication of three- dimensional woven textile preforms for composites. Textile Research Journal. 2011;**81**:932-944. DOI: 10.1177/0040517510392471

[10] Redman C, Bayraktar H, Mcclain M. Curved Beam Test Behavior of 3D Woven Composites. SAMPE Conf; 2014

[11] Bayraktar H, Ehrlich D, Goering J, Mcclain M, Composites AE, Hampshire N, et al. 3D Woven Composites for Energy Absorbing. 20th Int. Conf. Compos. Mater., Copenhagen; 2015. pp. 19-24

[12] EL-Dessouky H, Snape A, Tew H, Scaife R, Modi DK, Kendall K, et al. Design, weaving and manufacture of a large 3d composite structure for automotive applications. 7th World Conf. 3D Fabr. their Appl. 3D Fabr. their Appl; 2016

[13] El-Dessouky HM, Snape AE, Turner JL, Saleh MN, Tew H, Scaife RJ. 3D weaving for advanced composite manufacturing: From research to reality. SAMPE. 2017;**2017**

[14] Hemrick JG, Lara-Curzio E, Loveland ER, Sharp KW, Schartow R. Woven graphite fiber structures for use in ultra-light weight heat exchangers. Carbon N Y. 2011;**49**:4820-4829. DOI: 10.1016/j.carbon.2011.06.094

[15] Jewell J, Kennedy R, Menard A. Full-scale LEAP Fan Blade-Out Rig Test Yields Outstanding Results; Advanced LEAP Fan Endurance Test Complete. CFM Power Flight; 2011

[16] ASTM-D3171. Standard test methods for constituent content of composite materials. ASTM International. 2010;**15**:1-6. DOI: 10.1520/D3529M-10.2

[17] Mahadik Y, Brown KAR, Hallett SR. Characterisation of 3D woven composite internal architecture and effect of compaction. Composites. Part A, Applied Science and Manufacturing. 2010;**41**:872-880. DOI: 10.1016/j.compositesa.2010.02.019